DOI: 10.13009/EUCASS2022-4496

On the matching between design specifications and payload-range efficiency of transport airplanes

*Alejandro Sanchez-Carmona, Emilio Pérez, Cristina Cuerno-Rejado, and Rodrigo Martínez-Val**
Universidad Politécnica de Madrid, Grupo de investigación "Diseño preliminar de aviones y drones"
ETSI Aeronáutica y del Espacio, Plaza del Cardenal Cisneros 3, 28040, Madrid, Spain.
**rodrigo.martinezval@upm.es*

Abstract
In the current scenario of commercial aviation, with growing activity, environmental constraints and technological development, thousands of new airplanes will be required during the next decades. These aircraft should be designed to offer the most efficient operation from all points of view: environment, airlines, passengers… The traditional design process aims at providing passenger capacity and range to cover all demands within the various market segments, but this approach could be far from being the most appropriate one. The research reported here focus on how a better matching between design conditions and actual operating utilisation might improve the overall performance.

1. Introduction

Commercial aviation has evolved since pioneer times to become one of the most astounding technological achievements of industrial society. Its capacity and productivity are still growing, and most air traffic predictions indicate a remarkable increase for the coming decades, with an overall passenger traffic expected to go up at a yearly pace around 3% [1–3]. To encompass this history of success, airplane performances have also greatly improved over the last decades, mainly due to developments in key technological areas such as aerodynamics, propulsion, structures, avionics, materials, flight procedures, etc. [4,5]. Furthermore, currently all around the world governments are aware of regulating about emissions of pollution gases into the atmosphere in order to reduce them in the future, which affects also to the aviation industry [6,7]. The current scenario combines growing activity, environmental constraints, and technological development. Many thousands of airplanes will be required in the next decades to replace obsolete aircraft and to offer suitable solutions of market flourishing.

On another side, airline routes, that define the airplanes to be built, are largely determined by the interaction of geographical, political, economic and social factors that provide the initial specifications for new designs: payload capacity (i.e. number of passengers), range with a given payload, length of airport runways, and the like [8–11]. In order to optimise these new designs from the environmental point of view, most fuel, and consequently most of the emissions, is burned in the cruise phase [12]. Thus, main research efforts are focused on optimising aircraft performances in that flight condition [13]. However, usually actual operations are deviated from this optimum point, so several studies deal with the emissions impact of operating out of this point [14].

Airplane design is a multidisciplinary activity involving various, progressively complex stages and numerous, conflicting specifications and requirements. In the conceptual design phase, albeit data and information are very scarce, the designer has to take many decisions that will deeply affect key variables and, thus, the final product. Two aspects have to be considered at such level are:

- the design point, i.e. the selection of the wing loading and the thrust over weight ratio, to fulfil cruise, take-off, landing and second segment climb requirements;
- and the operating point, a specific payload-range pair within the foreseen payload-range (*PL-R*) diagram of the aircraft to match the most demanded routes and to offer adequate performances in all others.

This operating point is far from the *PL-R* envelope, on where the design point is located. The current aircraft are designed trying to cover the most part of the market, although just a few percent of flight will need to use the full capability of the aircraft [15]. Thus, the design point is on the segment of the *PL-R* diagram limited by maximum take-off weight, usually close to the maximum productivity point, which is the product of the payload and the range. However, this goal function, productivity, does not take into account the fuel consumption. Thence, some authors propose another parameter to consider also the effect of the fuel, which is the payload – range efficiency: the ratio of the product of the range and the payload in the numerator to mission fuel in the denominator [16].

DOI: 10.13009/EUCASS2022-4496

In this paper it is proposed to use *PL-R* efficiency to measure the effectiveness of the operation and analysing the effect of getting closer design and operating points in that variable. To undertake this study, first it is presented a methodology to size aircraft in section 2. Taking into account this model, the final expression for *PL-R* efficiency is presented in section 3. By means of the proposed methodology two different markets are going to be analysed, corresponding to a short range – single aisle aircraft and a long range – wide body one. Additionally, to allow the comparison between design and operating points, in section 4 it is presented a model of the more frequent flights of the market based on statistics collected for both cases object of this study. Finally, the comparison in terms of *PL-R* efficiency is performed between two aircraft, for each market, designed one with the classical initial specifications and the other reducing the design range trying to get closer design and operating points.

2. Conceptual aircraft sizing

Before starting this study, it is necessary to establish a methodology to carry out the preliminary sizing of aircraft. It allows the authors to analyse how the efficiency of the operation changes when the input variables also do it. The proposed procedure is based on first and second order methods to determine the main variables that are involved in the performance of the aircraft, such as maximum take-off weight, operative empty weight, or trip fuel. The independent input variables in the present methodology, which need to be decided by the designer, are payload and range. That is, the designer must define the design trip and, by means of this methodology, the aircraft is sized.

The take-off weight (*TOW*) is the addition of the operative empty weight (*OEW*), payload (*PL*), trip fuel (*TF*), and the reserve fuel (*RF*) [17–19]:

$$\mathbf{TOW = OEW + PL + TF + RF} \tag{1}$$

The maximum take-off weight (*MTOW*) is obtained when the corresponding values for the design trip are employed in Eq. (1). Obviously, *MTOW* cannot be smaller than the result provided by Eq. (1), because this would imply that the airplane could not perform the design trip. On the contrary, if *MTOW* is higher than the result obtained, the aircraft would be oversized for the design operation.

The operative empty weight is commonly estimated as a fraction of the maximum take-off weight:

$$\mathbf{OEW = f_e MTOW} \tag{2}$$

where the fraction parameter, f_e, is a function of the design range, R_d (in km), as follows [15]:

$$\mathbf{f_e = 0.6 - \frac{R_d}{100000}} \tag{3}$$

The reserve fuel is required to consider any contingency and/or to be capable of reaching an alternate airport. To simplify the methodology, this variable has been fixed as 5 percent of the landing weight (*LW*) [17,18]:

$$\mathbf{RF = 0.05LW} \tag{4}$$

The landing weight includes the operative empty weight, the payload, and the reserve fuel itself (see Eq. (4)):

$$\mathbf{LW = OEW + PL + RF} \tag{5}$$

Substituting Eq. (4) into Eq. (5):

$$\mathbf{LW = \frac{OEW+PL}{0.95}} \tag{6}$$

The trip fuel consumed by the aircraft depends on the range (*R*). Otherwise, the range of the aircraft can be estimated as follows [15]:

DOI: 10.13009/EUCASS2022-4496

$$\mathbf{R = 300 + K\ln\frac{0.975TOW}{1.02LW}} \tag{7}$$

The previous equation relies on the assumptions that the aircraft burns fuel as to 0.025 *TOW* during take-off and climb phases and that the burnt fuel along the descending and landing phases is roughly 2 per cent of the landing weight. Additionally, the distance travelled before and after the cruise phase has been approximated by 300 km. Finally, the range parameter *(K*) is the best representative of the overall aircraft performance [20]. Its value can be established a priori, as a first approximation, depending on the airplane category to which the aircraft belongs to.

Regarding the maximum payload of the aircraft, the present model considers that the quotient between the design payload and the maximum payload remains similar among aircraft of the same market segment. Furthermore, the maximum fuel weight of the aircraft is also determined considering that the ratio between its value and the maximum take-off weight is approximately constant for aircraft with similar design specifications. This set of magnitudes provide a first estimation of the payload–range diagram, making use of Equation 7 [21]. An example of the final *PL – R* diagram obtained is showed in Figure 1.

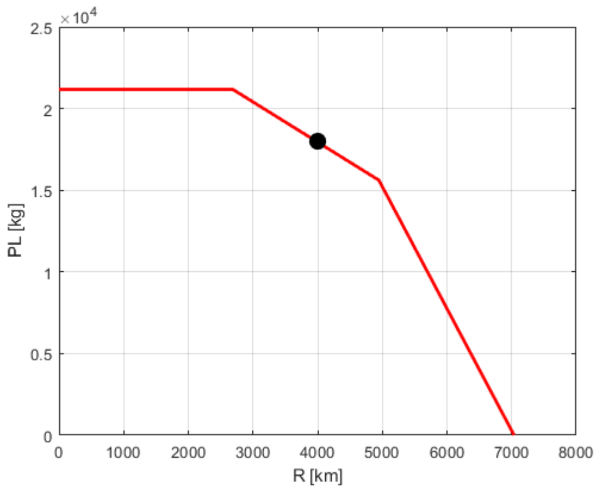

Figure 1: Payload – range diagram obtained for K = 25500 km, R_d = 4000 km, and PL_d = 18000 kg.

To sum up, once the design trip is chosen, by means of the corresponding values of design range and payload, and making use of all former equations, it is possible to determine the main variables which describe the aircraft, specifically, the maximum take-off weight and the trip fuel.

3. Operational effectiveness

Nowadays, the effectiveness of an aircraft cannot only be measured through the product of the payload by the range, which is usually called productivity. This variable refers to the aircraft capacity to generate revenues to the airline [11]. However, as the current regulation framework is severely constrained by the goal of reducing emissions, it should be desirable to measure the effectiveness of an aircraft taking into account also the fuel burn during the trip, as emissions are directly proportional to fuel consumption [22,23]. So, the model uses the ratio between productivity and trip fuel, ($PL\cdot R$)/TF, as the payload-range efficiency variable in this work.

The final objective of this research is to analyse the impact of the design variables in the *PL-R* efficiency along the whole payload–range diagram. Taking this into account, this section is devoted to determining how the goal function depends on the payload and the range. Starting by the trip fuel, it is possible to reach the following expression from Eqs. 6 and 7:

$$\mathbf{TF = TOW - LW = LW\left(\frac{1.02}{0.975}e^{\frac{R-300}{K}} - 1\right) = \frac{OEW+PL}{0.95}f_R} \tag{8}$$

where f_R is a function of the range:

DOI: 10.13009/EUCASS2022-4496

$$\mathbf{f_R} = \frac{1.02}{0.975}\mathbf{e}^{\frac{R-300}{K}} - \mathbf{1} \tag{9}$$

The final equation for the *PL-R* efficiency is, consequently:

$$\frac{\mathbf{PL \cdot R}}{\mathbf{TF}} = \frac{\mathbf{0.95PL}}{\mathbf{OEW+PL}}\frac{\mathbf{R}}{\mathbf{f_R}} \tag{10}$$

As it can be deduced from Eq. (10), the *PL-R* efficiency is a product of a function that only depends on the payload by another that only depends on the range, once the operative empty weight and the range parameter are determined. The function depending on the payload grows monotonously with the payload. On the other hand, the function depending on the range has a maximum for a determined value of range, as it is showed in Figure 2.

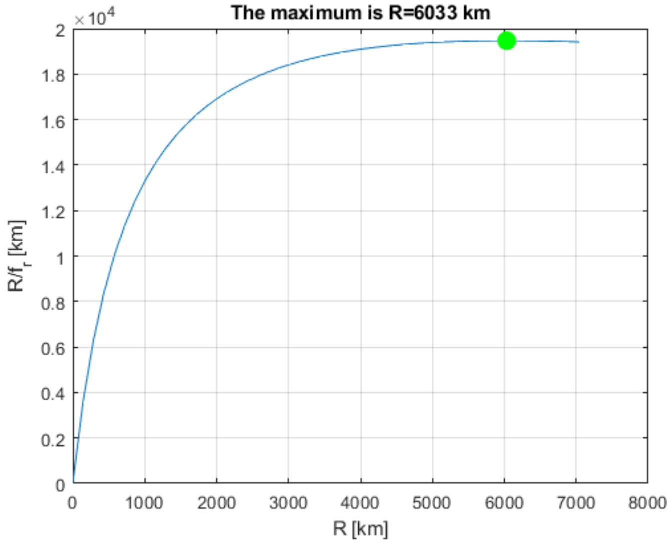

Figure 2: Behaviour of the function R/f_R for a range parameter of 25500 km.

Thus, the maximum *PL-R* efficiency, neglecting the constraints introduced by the *PL-R* diagram, would be reached for the optimum range shown in Figure 2 and the highest possible payload. When the diagram constraints are considered, the maximum always lies at the boundary of the payload–range diagram. The actual maximum will be at the tangent point of the constant *PL-R* efficiency curves, taking the highest value as possible. Depending on where this point is, it could coincide with the optimum range without any restrictions, or not.

4. *PL-R* probability distributions of the market

As the objective of the work is to compare the effectiveness of an aircraft between the design point and the most frequent *PL-R* point in commercial operations of the aircraft, this section develops how the *PL-R* probability distributions of the market have been modelled. To do that, two relevant markets have been analysed: long range – wide body and short range – single aisle. One aircraft representative of long range – wide body segment is Boeing 777. On the other hand, Airbus 320 has been taken as a typical aircraft of short range – single aisle segment. In the open literature, it is possible to find statistics that show how these two aircraft have been utilised in terms of range and payload along thousands of flights.

Focusing on B777, detailed information about landing weight and range is available for more than ten thousand flights from one carrier [24]. These data are represented as cumulative probability distributions (Figure 3 and Figure 4), i.e., percentage of flights with higher values than that of the corresponding abscissa variable, which are, respectively, landing weight and range. Such functions can be approximated by normal distributions. Regarding the weight, the mean and the standard deviation of the modelled distribution are obtained by maximising the coefficient of determination. In the case of the range, the actual data are approximated by a linear combination of two normal distributions, one that fits short-range flights and another for longer operations. The first fraction, that of short flights, represents 15% of total, with a mean of 545 km. The second normal distribution exhibits a mean of some 6000 km.

DOI: 10.13009/EUCASS2022-4496

The corresponding standard deviations are obtained, again, by maximising the coefficient of determination. The results obtained in this modelling process are indicated in Table 1.

Table 1: Normal distribution approximation for *LW* and *R* for B777-200ER.
Data for range include both means and both standard deviations.

	Mean	**Standard deviation**	**Coefficient of determination**
Landing weight	184 ton	10.12 ton	0.9998
Range	545, 6000 km	463, 1369 km	0.9959

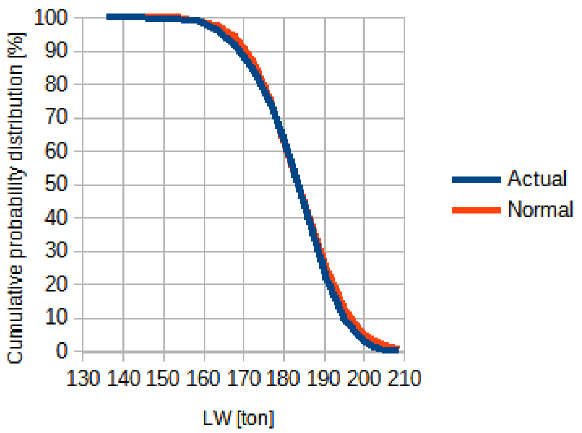

Figure 3: Actual statistics (dark blue line) of more than 10,000 flights for B777-200ER [24] and normal approximation (red line) for *LW*.

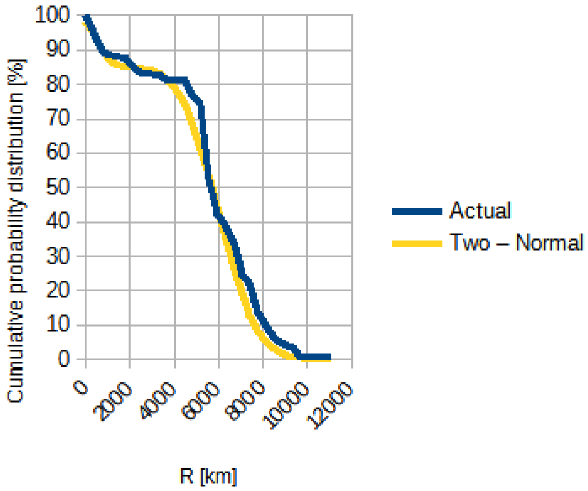

Figure 4: Actual statistics (dark blue line) of more than 10,000 flights for B777-200ER [24] and linear combination of normal distributions approximation (yellow line) for range.

Analogously, it is possible to model the representative short range – single aisle aircraft. Similar statistics than those for B777 have been found for A320, again corresponding to more than ten thousand flights [25]. Figures 5 and 6 show the cumulative probability distributions obtained for landing weight and range. As previously done for the larger

DOI: 10.13009/EUCASS2022-4496

aircraft, the normal approximations are also represented in these plots. The procedure followed to obtain the parameters which define the normal distribution is the same than that described in B777. In analysing range statistics, the appearance is newly the sum of two markets, one for rather short flights and, another, for longer range routes. Here the change in the behaviour of the curve is around 60% of the cumulative probability distribution. Thus, it is assumed that the normal distribution which fits the short-range flights encompasses the 40% of the flights. Consequently, the long-range normal distribution represents the other 60% of the flights. The means of both distributions have been taken from the corresponding interval where they are applied. Both standard deviations have been found by maximising the coefficient of determination. The results are included in Table 2

Table 2: Normal distribution approximation for *LW* and *R* for A320-200.
Data for range include both means and both standard deviations.

	Mean	**Standard deviation**	**Coefficient of determination**
Landing weight	58.89 ton	4.02 ton	0.9985
Range	1118, 3158 km	398, 748 km	0.9965

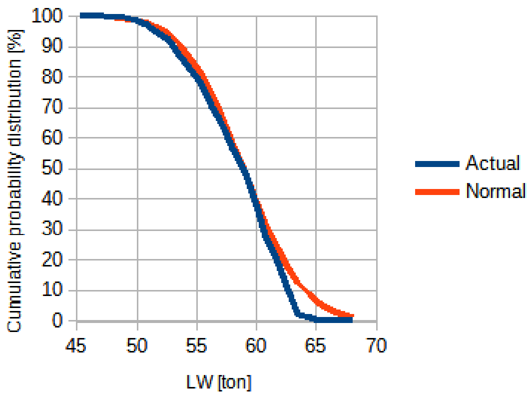

Figure 5: Actual statistics (dark blue line) of more than 10,000 flights for A320-200 [25]
and normal approximation (orange line) for *LW*.

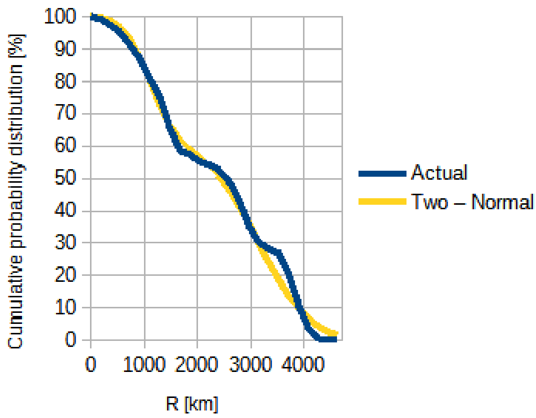

Figure 6: Actual statistics (dark blue line) of more than 10,000 flights for A320 [25]
and linear combination of normal distributions approximation (yellow line) for range.

Once these models have been presented and validated, the use for this work is to find where the points of maximum operation frequency are located inside the *PL-R* diagram. The range distribution can be taken directly. The payload distribution is obtained from the landing weight distribution. As the operative empty weight is known and the percentage of reserve fuel with respect to the landing weight can be taken as 5%, payload weight can be estimated

DOI: 10.13009/EUCASS2022-4496

directly from landing weight. At this point, it is assumed that the two distribution functions, range, and payload, are independent to each other. In consequence, it is possible to build a two-dimension distribution function which represent the aircraft utilization in terms of range and payload, as the product of the range distribution function and the payload one. This procedure is undertaken for both flight segments, and the resulting functions are represented in Figs 7 and 8. In each figure, there are two points to highlight, which corresponds to the two means of the normal distributions that build the model. These points are considered as the maximum frequency points, despite the shorter range case has a higher probability in the narrow body aircraft, the contrary as the long range – wide body case. It is remarkable that some of the market is out of the *PL-R* diagram in both cases. This is caused by the fact that the performances of the designed aircraft do not coincide exactly with those selected to build the statistical models for A320 and B777. Despite these mismatches, both models can be taken as representative of the market in both flight segments.

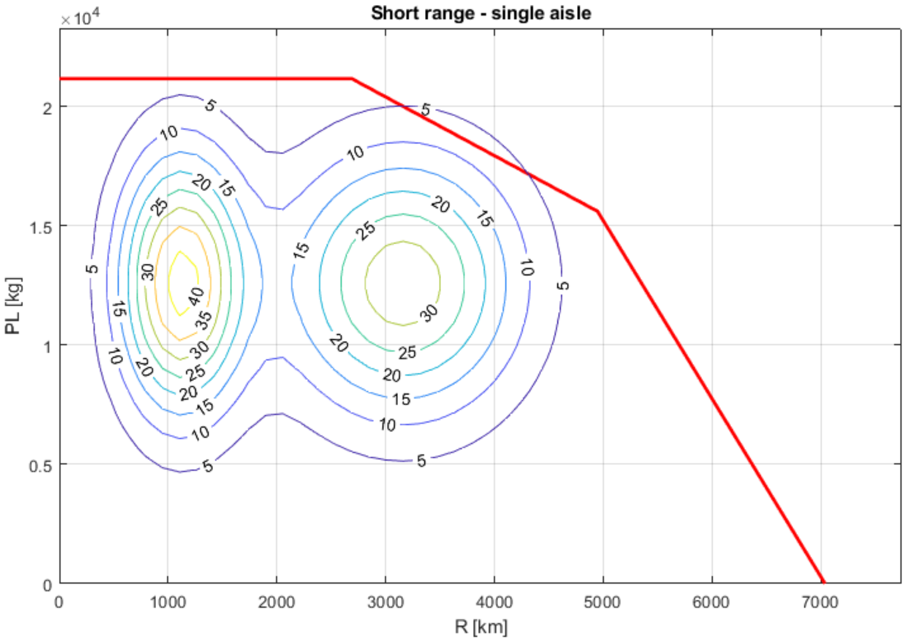

Figure 7: Final model for aircraft use frequency for single aisle aircraft obtained with K = 25500 km, PL_d = 18000 kg, and R_d = 4000 km. The level curves represent the values of the probability density function multiplied by 10^9.

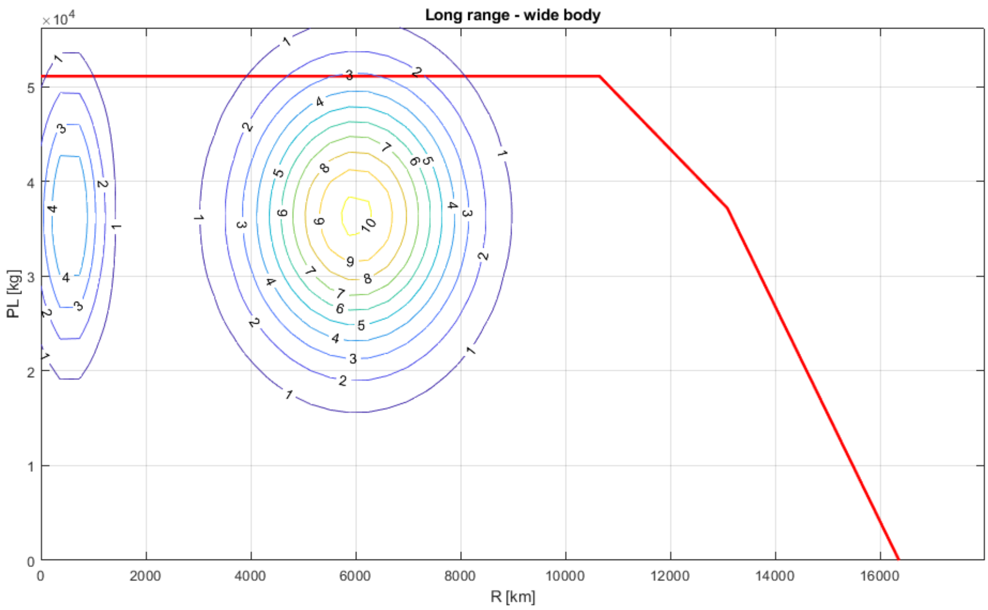

Figure 8: Final model for aircraft use frequency for wide body aircraft obtained with K = 31000 km, PL_d = 37000 kg, and R_d = 13000 km. The level curves represent the values of the probability density function multiplied by 10^9.

DOI: 10.13009/EUCASS2022-4496

5. Results

Once the *PL-R* efficiency has been presented, the procedure for sizing aircraft has been described, and how the *PL-R* probability distribution is modelled from market's data, it is time to analyse that efficiency through some relevant points inside the *PL-R* diagram, such as maximum frequency points, design points, and maximum efficiency points. This analysis will be performed separately for the two market segments considered: short range – single aisle and long range – wide body, since the frequency distribution functions are quite different to each other.

The results are presented in Figure 9. The graphs show the *PL-R* diagram with red lines and the relevant points described former, where blue points are the maximum frequency points, black points are the design points, and yellow points are the maximum effectiveness points reached inside the diagram. Furthermore, the background colour refers to different levels of *PL-R* effectiveness. Remember that the maximum effectiveness is reached for the highest possible payload and for a specific range.

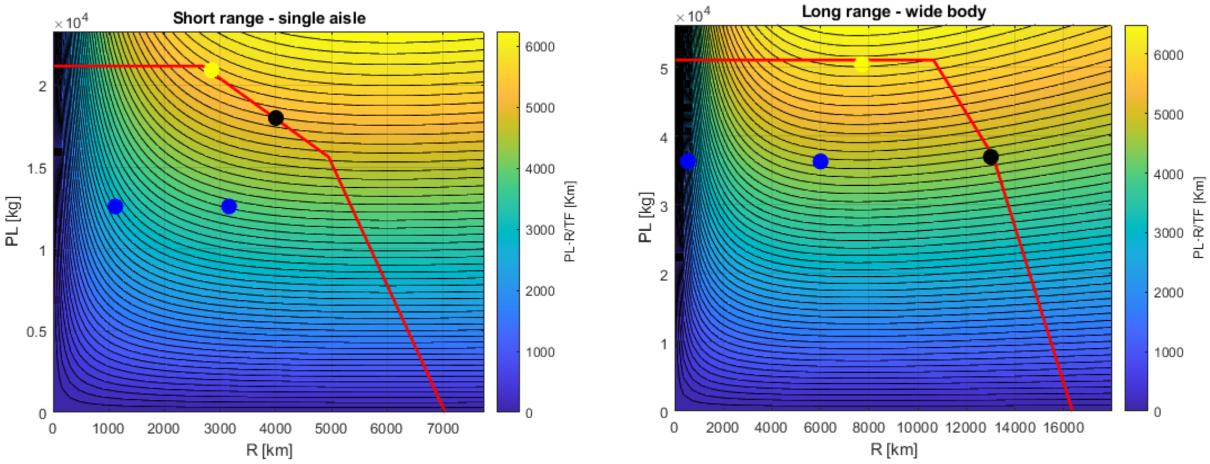

Figure 9: *PL-R* effectiveness for short range – single aisle aircraft (left) and long range – wide body aircraft (right). The diagram on the left is obtained with K = 25500 km, PL_d = 18000 kg, and R_d = 4000 km, and that on the right with K = 31000 km, PL_d = 37000 kg, and R_d = 13000 km. The level curves represent the *PL-R* efficiency, according to the colour code shown to the right of both plots.

Focusing on the single aisle aircraft, the optimum range, neglecting the diagram's constraints, is at 6033 km. This point lies beyond the PL-R envelope, particularly, above the constraint defined by maximum fuel weight. In consequence, when considering the points inside the diagram, the maximum *PL-R* efficiency is reached in the intersection between the *MPL* and *MTOW* constraints (yellow dot), because that is where one *PL-R* efficiency curve is tangent to the *PL-R* diagram. This point is rather far from the design point (black dot) and from the two maximum frequency points defined for this market segment (blue dots). With respect to wide body aircraft case, the optimum range is at 7676 km. In this scenario, the point belongs to the maximum payload constraint of the diagram (yellow dot). In both diagrams, the range corresponding to maximum *PL-R* efficiency is closer to the greatest mean range extracted from the market (Tables 1 and 2) than to the shortest one, even though for single aisle aircraft the shortest flights cumulate higher probability density. Another interesting comment is that the payload commonly taken onboard narrow body airplanes is smaller than that of the design point, which does not occur for the wide body where the design and actually flown payloads are about the same.

After presenting these results, a reflection emerges: would it be possible to improve the *PL-R* efficiency in the surroundings of maximum frequency of operation points? Should this be possible, aircraft would fly in more environmentally friendly conditions. To achieve this goal, the design point should be closer to the maximum frequency point. However, there is a trade-off between maximising the efficiency and covering as much market as possible. From Figures 7 and 8, the percentage of market out of the *PL-R* diagram in the two considered aircraft are 2.85% and 6.23%, for single aisle and wide body aircraft, respectively. This probability corresponds to the volume of the modelled probability density function, which depends on range and payload, that falls out of the diagram. The proposal is, then, to reduce the range of the design point to be closer to the maximum flight frequency points and observe how the *PL-R* efficiency improves. To separate the blurring produced by modifying two variables simultaneously, this proposal holds the payload of the design point, so *MPL* of the aircraft is kept and, consequently, the fuselage is exactly the same.

DOI: 10.13009/EUCASS2022-4496

In order to choose a new design point assuring that most the market falls inside the *PL-R* diagram, it is essential to depict the statistical distribution of flights within the diagram. In the case of single aisle aircraft, if the design point is taken as the range that equals the shorter maximum frequency point plus one standard deviation, the resulting diagram becomes that of Figure 10. That result implies that around 15.4% of the market cannot be serviced by this airplane. On considering the wide body aircraft, defining the design range as that of the maximum frequency plus 1.5 times the standard deviation, the percentage of market that is lost is slightly larger, 16.1%.

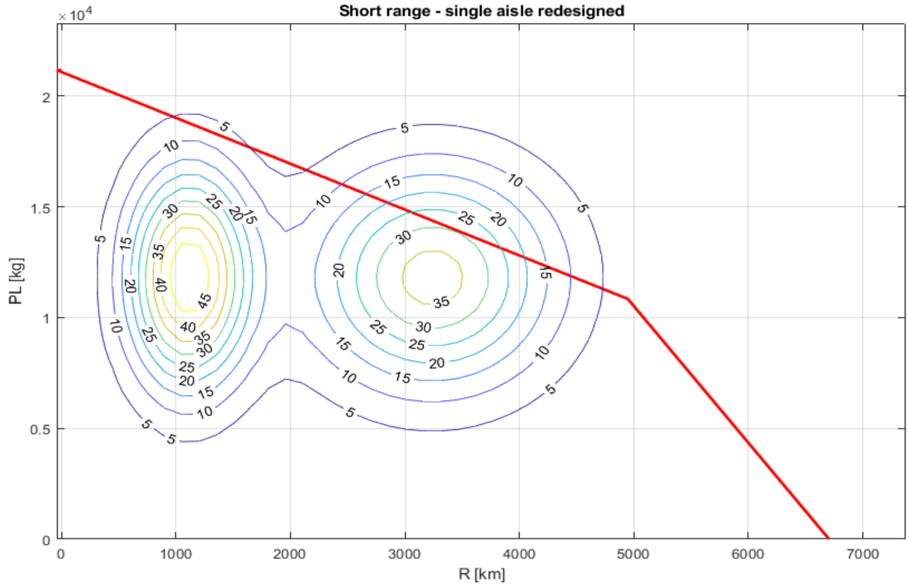

Figure 10: Model for aircraft frequency of use for short range – single aisle aircraft obtained with K = 25500 km, PL_d = 18000 kg, and R_d = 1481.6 km. Level curves of probability density function multiplied by 10^9.

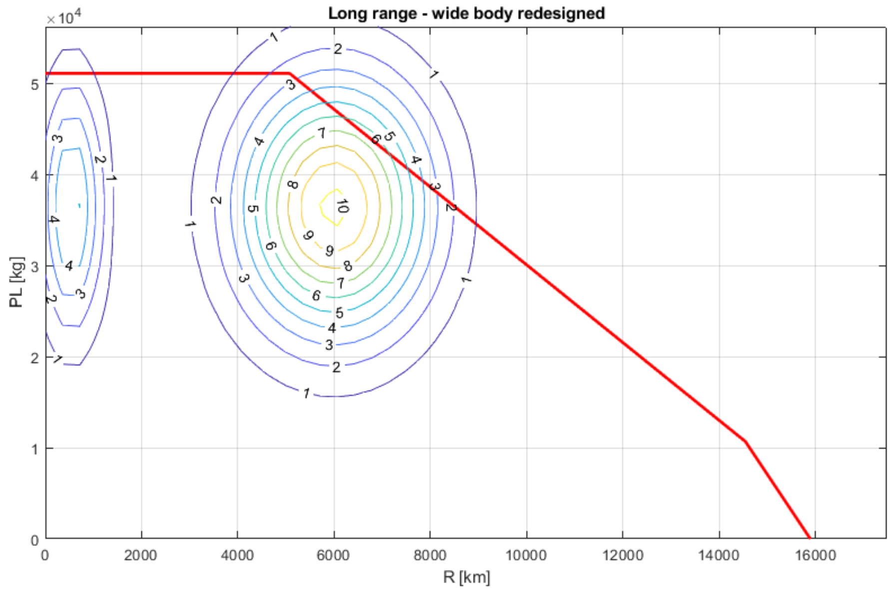

Figure 11: Model for aircraft frequency of use for long range – wide body aircraft obtained with K = 31000 km, PL_d = 37000 kg, and R_d = 8053.4 km. The level curves as in Fig. 10.

Thus, it is now possible to compare the *PL-R* effectiveness in the maximum frequency points defined by the market between the aircraft obtained with classical design points and with the new design points proposed in the present study. Figure 12 shows the results for narrow and wide bodies. The short range – single aisle aircraft has now its maximum

DOI: 10.13009/EUCASS2022-4496

effectiveness point over the boundary defined by the *MTOW* limitation. Nevertheless, the *PL-R* efficiency is higher in the surroundings of the maximum frequency points. Regarding the long range – wide body aircraft, the maximum effectiveness point is in the intersection between the constraints defined by *MTOW* and *MPL*. However, as it happens for the narrow body case, the efficiency increases around the maximum frequency point. Table 3 presents the efficiency reached at these points. The improvement in the short-range aircraft is near 10%, in both maximum frequency points. On the other hand, in long-range aircraft the *PL-R* efficiency increases more than 20% in both maximum frequency points. Therefore, the proposed strategy to take the design point closer to the maximum frequency ones leads to much better performance in both cases considered.

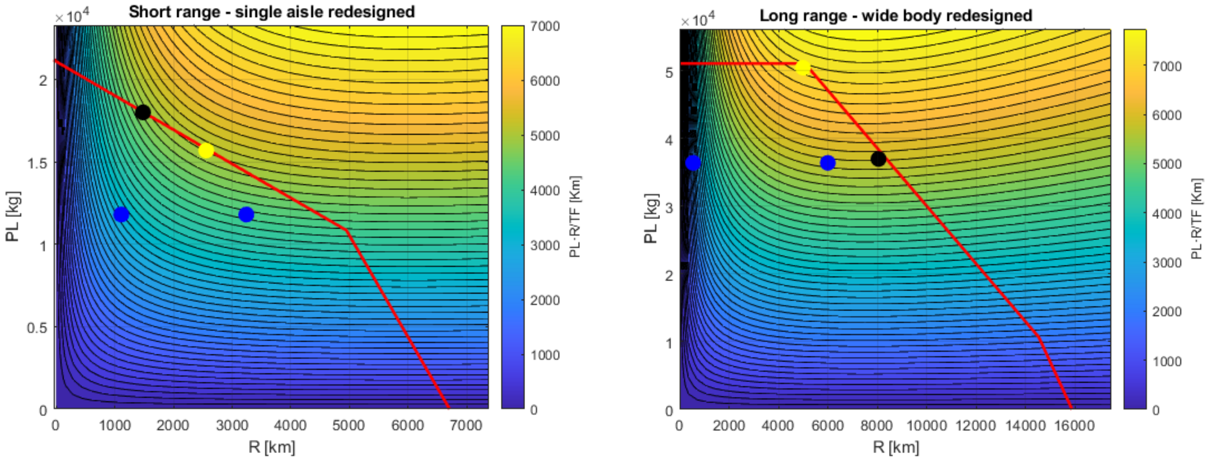

Figure 12: *PL-R* efficiency for short range – single aisle aircraft (left) and long range – wide body aircraft (right). The left diagram is obtained with K = 25500 km, PL_d = 18000 kg, and R_d = 1481.6 km, and the right diagram with K = 31000 km, PL_d = 37000 kg, and R_d = 8053.4 km. Level curves as in Figure 9.

Table 3: *PL-R* efficiency, in kilometres, of maximum frequency points.

	First point	Second point
Short range – single aisle	2922	3892
Short range – single aisle redesigned	3194	4280
Long range – wide body	2040	4752
Long range – wide body redesigned	2494	5809

6. Conclusions

This work deals with the idea of using (*PL•R)*/*TF* as a parameter to measure the efficiency of aircraft operations. It is shown that this parameter can be expressed as a multiplication of two functions, one dependent on payload weight and operative empty weight and another depending on range parameter and the range itself. The maximum *PL-R* efficiency is reached for a specific value of range. However, it increases monotonically with respect to the payload. Thus, the maximum efficiency is always reached at the contour of the *PL-R* diagram.

A model of aircraft frequency of use has been presented for two market segments: short range – single aisle and long range – wide body. The studied market that represents the first segment behaves as a linear combination of two normal distributions in terms of range. On the contrary, the range of the analysed flights of the second segment can be modelled as a simple normal distribution. Additionally, the payload weight has been studied along a wide set of flights for both market segments, and the conclusion is that both can be approximated through normal distributions. The main conclusion of this analysis is that the maximum frequency points are always well inside the *PL-R* diagram, far from its envelope, in both cases, and far from the corresponding maximum efficiency points.

DOI: 10.13009/EUCASS2022-4496

As a main result of the research reported here, it has been proposed to design future aircraft with design points closer to maximum frequency points. This design philosophy consists of reducing the range of the design point while keeping the original payload weight, which is paired to the fuselage sizing. Although after this new design approach the maximum efficiency points and the maximum frequency points will not coincide neither, on comparing the *PL-R* efficiency reached in the surroundings of the maximum frequency points between aircraft designed in the conventional way and those with shorter design ranges, it can be observed that the efficiency is clearly higher in this second situation. The proposed approach would imply that some market could not be covered, but most of the aircraft would fly in a much more efficient way in terms of fuel consumption and emissions.

References

[1] Federal Aviation Administration. 2021. *FAA Aerospace Forecast Fiscal Years 2021-2041*. FAA report.

[2] Boeing. 2021. *Commercial Market Outlook 2021 – 2040*. Boeing report.

[3] Airbus. 2021. *Airbus Global Market Forecast 2021 - 2040*. Airbus report.

[4] Anderson, J. D. 2002. *The Airplane: A History of Its Technology*. Reston, VA, USA, AIAA.

[5] Martinez-Val, R., and Perez, E. 2009. Aeronautics and Astronautics: Recent Progress and Future Trends. *Proceedings of the Institution of Mechanical Engineers, Part C: Journal of Mechanical Engineering Science*, Vol. 223, No. 12, pp. 2767–2820.

[6] ACARE (The Advisory Council for Aeronautics Research in Europe). 2010. *Aeronautics and Air Transport Beyond Vision 2020 (Towards 2050)*. European Commission, Brussels.

[7] European Parliament, C. of the E. U. 2009. Directive 2008/101/EC of the European Parliament and of the Council of 19 November 2008 Amending Directive 2003/87/EC so as to Include Aviation Activities in the Scheme for Greenhouse Gas Emission Allowance Trading within the Community. *Official Journal of the European Union*, Vol. 52, No. L8, pp. 3–21.

[8] Chai, X., Yu, X., and Wang, Y. 2018. Multipoint Optimization on Fuel Efficiency in Conceptual Design of Wide-Body Aircraft. *Chinese Journal of Aeronautics*, Vol. 31, No. 1, pp. 99–106.

[9] Yoon, J., Nguyen, N. Van, Choi, S. M., Lee, J. W., Kim, S., and Byun, Y. H. 2010. Multidisciplinary General Aviation Aircraft Design Optimizations Incorporating Airworthiness Constraints. *10th AIAA Aviation Technology, Integration and Operations Conference 2010, ATIO 2010*, Vol. 3.

[10] Clark, P. 2007, *Buying the Big Jets : Fleet Planning for Airlines*. Abingdon, UK, Ashgate.

[11] Morrell, P. S. 2007. *Airline Finance*. Abingdon, UK, Ashgate.

[12] Singh, V., and Sharma, S. K. 2015. Fuel Consumption Optimization in Air Transport: A Review, Classification, Critique, Simple Meta-Analysis, and Future Research Implications. *European Transport Research Review*, Vol. 7, No. 2.

[13] Lyu, Y., and Liem, R. P. 2020. Flight Performance Analysis with Data-Driven Mission Parameterization: Mapping Flight Operational Data to Aircraft Performance Analysis. *Transportation Engineering*, Vol. 2.

[14] Poll, D. I. A. 2018. On the Relationship between Non-Optimum Operations and Fuel Requirement for Large Civil Transport Aircraft, with Reference to Environmental Impact and Contrail Avoidance Strategy. *The Aeronautical Journal*, Vol. 122, No. 1258, pp. 1827–1870.

[15] Martinez-Val, R., Roa, J., Perez, E., and Cuerno, C. 2011. Effects of the Mismatch between Design Capabilities and Actual Aircraft Utilization. *Journal of Aircraft*, Vol. 48, No. 6, pp. 1921–1927.

[16] Kaivanto, K., and Zhang, P. 2018. A Fuel-Payload Ratio Based Flight-Segmentation Benchmark. *Transportation Research Part D: Transport and Environment*, Vol. 63, pp. 548–559.

[17] Torenbeek, E. 1982. *Synthesis of Subsonic Airplane Design*. Dordrecht (NL), Springer Netherlands.

[18] Roskam, J. 1989. *Airplane Design, Part II : Preliminary Configuration Design and Integration of the Propulsion System*. Ottawa, KS, USA, Roskam Aviation and Engineering Corporation.

[19] Raymer, D. P. 2012. *Aircraft Design: A Conceptual Approach*. Sylmar, CA, USA, AIAA Education Series.

[20] Martinez-Val, R., Palacin, J. F., and Perez, E. 2008. The Evolution of Jet Airliners Explained through the Range Equation. *Proceedings of the Institution of Mechanical Engineers, Part G: Journal of Aerospace Engineering*, Vol. 222, No. 6, pp. 915–919.

[21] Martínez-Val, R., Pérez, E., Munoz, T., and Cuerno, C. 1994. Design Constraints in the Payload-Range Diagram of Ultrahigh Capacity Transport Airplanes. *Journal of Aircraft*, Vol. 31, No. 6, pp. 1268–1281.

[22] Wasiuk, D. K., Khan, M. A. H., Shallcross, D. E., and Lowenberg, M. H. 2016. A Commercial Aircraft Fuel Burn and Emissions Inventory for 2005-2011. *Atmosphere*, Vol. 7, No. 6, pp. 1–14.

[23] Głowacki, P., and Kawalec, M. 2015. Aircraft Fuel Consumption and Emissions During Cruise, Effect of the Jet Stream. *Journal of KONES. Powertrain and Transport*, Vol. 22, No. 2, pp. 63–78.

[24] DO, T., DA, S., JW, R., Jones, T., and DA, H. 2006. Statistical Loads Data for the Boeing 777-200ER Aircraft in Commercial Operations. Vol. DOT/FAA/AR, pp. 1–104.

[25] DO, T., DA, S., JW, R., Jones, T., and DA, H. 2006. Statistical Loads Data for the Airbus A-320 Aircraft in Commercial Operations. Vol. DOT/FAA/AR, pp. 1–104.